AD-A257 371

An Automated System for Measuring Velocity Distribution in Cesium Beam Tubes

Prepared by

S. K. KARUZA, W. A. JOHNSON, M. F. BOTTJER,
and F. J. VOIT
Communications Systems Subdivision
Electronics and Sensors Division

and

J. P. HURRELL
Electronics Technology Center
Technology Operations

30 September 1992

DTIC
ELECTE
NOV 12 1992
S E D

92-29318

THE AEROSPACE CORPORATION
El Segundo, California

92 11 10 030

QUANG BUI, Lt, USAF
MOIE Program Manager

CYNTHIA B. TENEROWICZ, 1Lt, USAF
Payload Development Engineer
GPS Space Segment

REPORT DOCUMENTATION PAGE
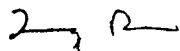
1a. REPORT SECURITY CLASSICATION Unclassified		1b. RESTRICTIVE MARKINGS		
2a. SECURITY CLASSIFICATION AUTHORITY		3. DISTRIBUTION/AVAILABILITY OF REPORT Approved for public release; distribution unlimited.		
2b. DECLASSIFICATION/DOWNGRADING SCHEDULE				
4. PERFORMING ORGANIZATION REPORT NUMBER(S) TR-0090(5925-08)-1		5. MONITORING ORGANIZATION REPORT NUMBER(S) SMC-TR-92-47		
6a. NAME OF PERFORMING ORGANIZATION The Aerospace Corporation Communications Systems Subdivision	6b. OFFICE SYMBOL (If applicable)	7a. NAME OF MONITORING ORGANIZATION Space and Missile Systems Center		
6c. ADDRESS (City, State, and ZIP Code) El Segundo, CA 90245		7b. ADDRESS (City, State, and ZIP Code) Los Angeles Air Force Base Los Angeles, CA 90009-2960		
8a. NAME OF FUNDING/SPONSORING ORGANIZATION	8b. OFFICE SYMBOL (If applicable)	9. PROCUREMENT INSTRUMENT IDENTIFICATION NUMBER F04701-88-C-0089		
8c. ADDRESS (City, State, and ZIP Code)		10. SOURCE OF FUNDING NUMBERS		
		PROGRAM ELEMENT NO.	PROJECT NO.	TASK NO.	WORK UNIT ACCESSION NO.

11. TITLE (Including Security Classification)
An Automated System for Measuring Velocity Distribution in Cesium Beam Tubes

12. PERSONAL AUTHOR(S)   Karuza, S. K.; Johnson, W., A.; Hurrell, J. P.; Bottjer, M. F.; Voit, F. J.

13a. TYPE OF REPORT	13b. TIME COVERED FROM _____ TO _____	14. DATE OF REPORT (Year, Month, Day) 30 September 1992	15. PAGE COUNT 23

16. SUPPLEMENTARY NOTATION

17.	COSATI CODES		18. SUBJECT TERMS (Continue on reverse if necessary and identify by block number)
FIELD	GROUP	SUB-GROUP	Cesium frequency standards, Cesium velocity distributions,
			Pulsed microwave technique

18. ABSTRACT (Continue on reverse if necessary and identify by block number)

This report describes a completely automated system for measuring the velocity distribution in a cesium (Cs) beam tube. The measurement system uses the short-pulsed microwave excitation method on Cs beam tubes having separated Ramsey-type interaction regions. This pulsed technique allows for the observation of signals that result from very narrow atomic-velocity groups. The brief theoretical operation of this method is discussed, after which the velocity distributions of six Cs beam tubes from four different manufacturers are presented. Data are presented that show the reproducibility of this measurement on the same beam tube, and comparisons among different tubes are made. Also, velocity distributions have been measured on all seven Zeeman transitions from one tube that exhibits small Rabi pulling. The knowledge of this Cs beam tube's velocity distribution provides considerable insight into the performance and alignment of the beam optics, and thus could be used for the diagnostic testing of Cs beam tubes. We have used this method to characterize a large number of such tubes.

20. DISTRIBUTION/AVAILABILITY OF ABSTRACT ☒ UNCLASSIFIED/UNLIMITED ☐ SAME AS RPT. ☐ DTIC USERS	21. ABSTRACT SECURITY CLASSIFICATION Unclassified	
22a. NAME OF RESPONSIBLE INDIVIDUAL	22b. TELEPHONE (Include Area Code)	22c. OFFICE SYMBOL

DD FORM 1473, 84 MAR   83 APR edition may be used until exhausted.   SECURITY CLASSIFICATION OF THIS PAGE
All other editions are obsolete.

Preface

This document was originally presented under the same title in *Proceedings of the 4th European Frequency and Time Forum* (Neuchâtel, Switzerland, 13-15 March 1990), pp. 555-563.

Accesion For		
NTIS CRA&I		☑
DTIC TAB		☐
Unannouiiced		☐
Justification		
By		
Distribution /		
Availability Codes		
Dist	Avail and / or Special	
A-1		

DTIC QUALITY INSPECTED 4

1

CONTENTS

FIGURES

TABLE

I. INTRODUCTION

Since the velocity distribution provides quantitative information about the alignment of the optics in a cesium (Cs) beam tube, and because this alignment in turn affects the final performance of the Cs frequency standard, there is a need to develop a system that measures this velocity distribution accurately. In order to minimize the data-taking time, it was decided to automate the measurement system. The early investigators [1,2,3] developed a method that used the pulsed excitation of atomic beam devices that had Ramsey-type interaction regions; this allowed for the observation of signals that were due to very narrow velocity groups.

Because the duty cycle of the pulsed microwave power is low, the current of the output beam is a small fraction of the current of the CW signal. A typical beam current output for the pulsed condition is about 0.06 nA. Therefore, long integration times are needed to measure the signals used to determine the velocity distributions. Measurements become time-consuming, and the accuracy and calibration of the measurement system itself become critical. Completely automating the measurement process drastically reduces the data-taking time. An additional advantage of automation is that one never has to make and remake the electrical connections.

Figure 1 shows the operation of the Ramsey cavity with pulsed microwave power. The velocity distribution of the beam tube detector cannot be inferred simply from the velocity distribution of the oven, because the beam optics will modify the oven's velocity distribution significantly, as shown in Figure 2. Figure 2 shows a typical beam-tube velocity distribution as measured at the detector, as well as the Maxwell-Boltzmann distribution created by the flux of atoms leaving the Cs oven. The shape of the velocity distribution provides information about the "optical" design and alignment of the tube, namely its reproducibility and its utilization of the Cs flux from the oven. When the velocity distribution is known, it is possible to calculate the second-order Doppler-shift correction for that particular beam tube; it is also possible to determine the cavity phase shift [1,2] from additional experimental data.

Some of the major factors affecting the width of the Cs tube's velocity distribution are as follows: (1) wider detector ribbons will lead to broader velocity distributions, (2) smaller misalignment of tube components increases the number of fast atoms detected, and (3) higher field state-selecting magnets allow for the improved collection of faster atoms. Changes in the velocity distribution with time may help to determine whether or not unwanted Cs deposits develop on sensitive apertures and thus contribute to background signals that degrade performance. This velocity distribution provides considerable insight into the performance of Cs clocks, because the Cs tube acts as a stable, very high-Q frequency discriminator that controls the long-term performance of the clock. The shape of this discriminator, as determined by the Ramsey resonance curve, is dependent upon the mean velocity and the moments of this velocity distribution.

A system has been designed and implemented to measure these velocity distributions precisely, using the pulse technique developed by Hellwig et al. [1].

5
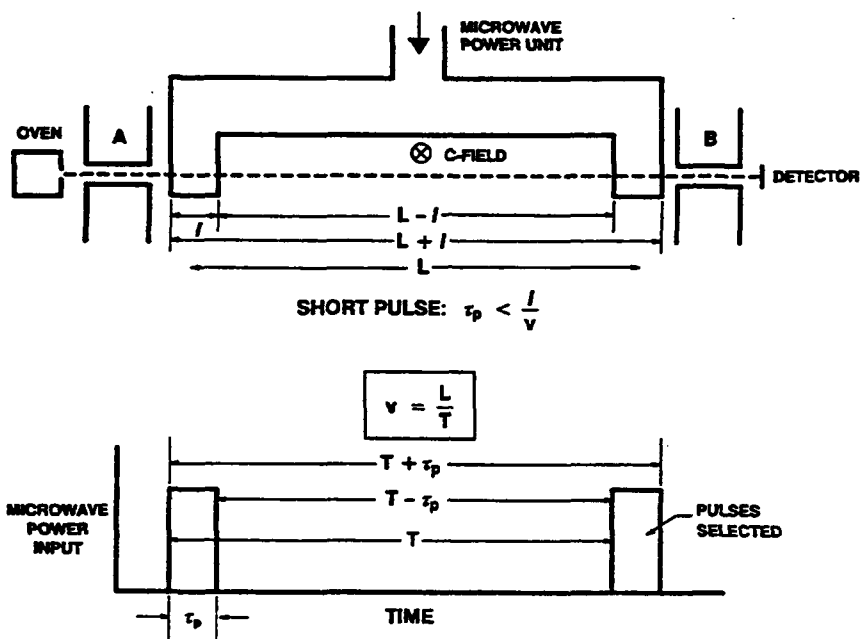
Figure 1. Operation of the Ramsey Cavity with Pulsed Microwave Power. The design of the Ramsey dual-interaction region permits one to select the velocity of the atomic beam by setting the period T of the microwave pulses.
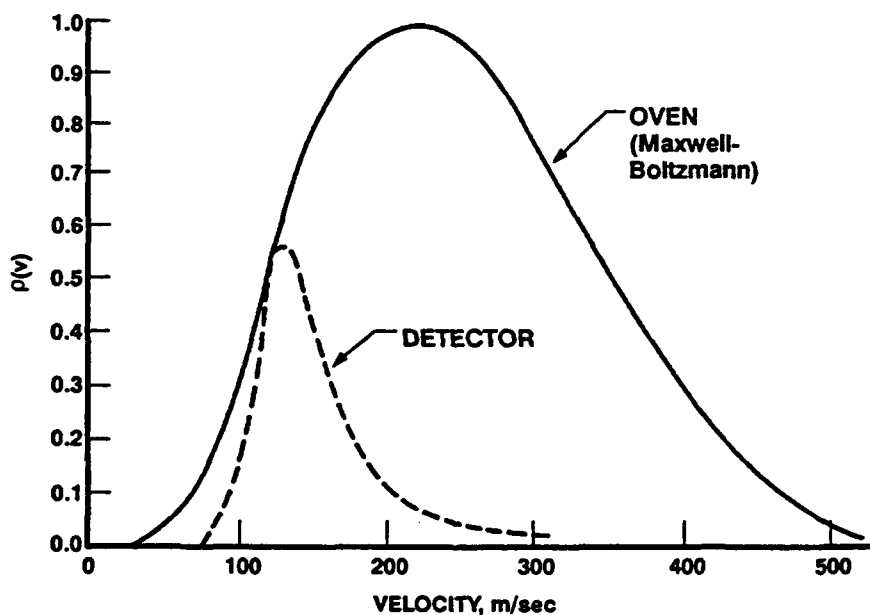

Figure 2. Cesium Beam Velocity Distribution. The Maxwell-Boltzmann velocity distribution out of the Cs oven is shown, along with the modified velocity distribution, selected by the beam optics, as measured at the detector.

6

II. MEASUREMENT TECHNIQUE

The interaction between the atomic beam and a pulsed microwave field occurs only for those few Cs atoms that are in the cavity interaction regions when the pulses occur. Since the time when the atoms interact with the microwave field has an uncertainty that is set by the length l of the single cavity region, there exists a velocity window Δv (see Figure 3) that varies with the pulse period T. The smaller the velocity window, the more precise will be the velocity measurement. Since most of the Cs atoms experience the microwave field in only one of the two separated cavity sections, the Ramsey resonance is small and is superimposed on a large Rabi pedestal. Figure 4 shows the spectrum for both CW and pulsed conditions. The widening of the Rabi pedestal is caused by the reduced interaction time τ_p.
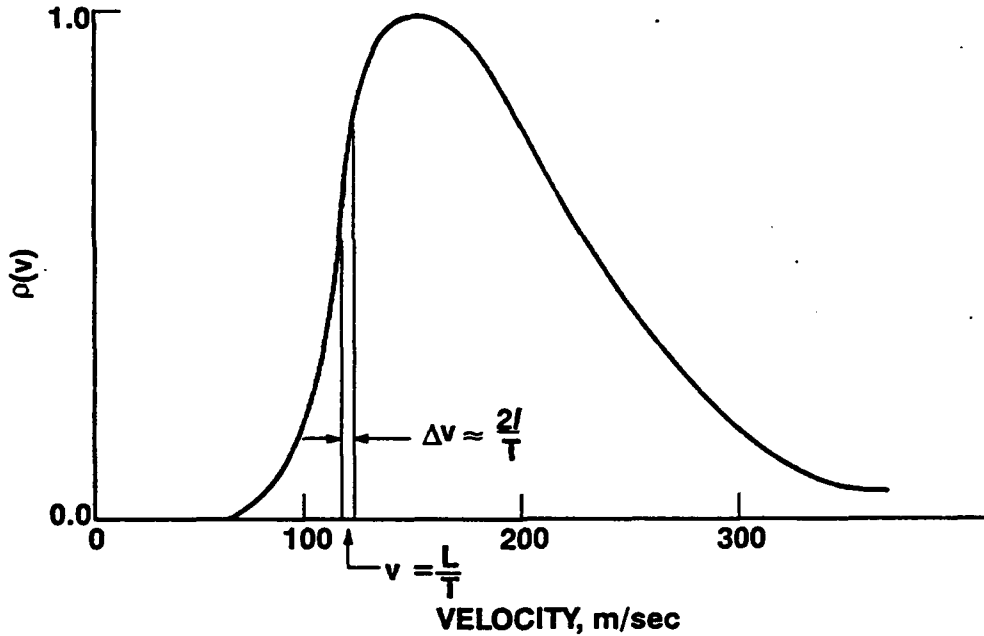
Figure 3. The Velocity Window Δv. The pulsed microwave power technique measures the flux of Cs atoms for a velocity window Δv.

For a pulse width τ_p and a pulse-repetition period T, there will be a narrow range of atomic velocities for which the atoms will experience resonance in both of the microwave interaction regions. It is clear from Figure 1 that the mean velocity v of these atoms is given by

$$v = \frac{L}{T} \; . \tag{1}$$

7
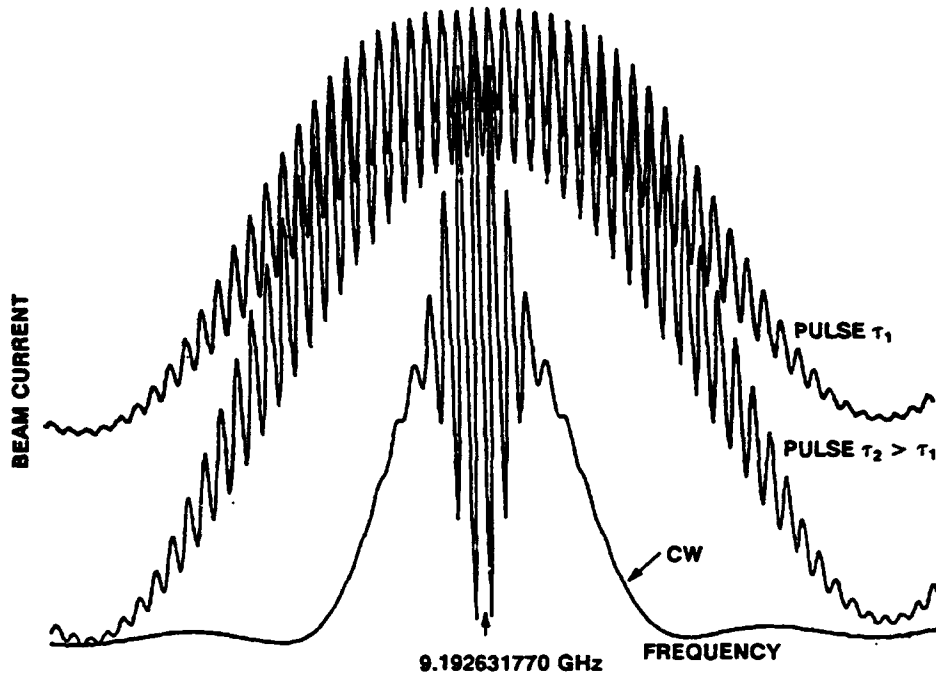
Figure 4. Ramsey Spectrum of the Cs Beam Tube under both Normal CW
Operation and the Pulsed Microwave Condition

The spectrum of the beam tube shown in Figure 4 is due to this class of atoms. The pulse width
τ_p is chosen so that

$$\tau_p < \frac{l}{v} = \frac{l}{L} \times T \ , \tag{2}$$

as noted in Figure 1.

In general, the fastest atoms in this ensemble will travel a distance $L + l$ in a time of approxi-
mately $T - \tau_p$; i.e., they will enter the left side of the left interaction region at the trailing edge of
the first pulse and will leave the right side of the right interaction region at the leading edge of the
next pulse. Then, if we call this fastest velocity v_f, we obtain

$$v_f(T - \tau_p) = L + l \ . \tag{3}$$

Similarly, the slowest atoms that will also experience resonance in both of the microwave
regions will leave the right side of the left interaction region at the leading edge of the first pulse
and will enter the left side of the right interaction region at the trailing edge of the second pulse.
Then, if we call this slowest velocity v_s, we obtain

$$v_s(T + \tau_p) = L - l \ . \tag{4}$$

The range of velocities Δv for which there is interaction in both regions is then

8

$$\Delta v \;=\; v_f - v_s \;=\; \frac{L+l}{T-\tau_p} - \frac{L-l}{T+\tau_p} \;\approx\; \frac{2l}{T}\left[1 + \left(\frac{L}{l}\right)\left(\frac{\tau_p}{T}\right)\right] \; . \tag{5}$$

Then, since $l < L$ and $\tau_p \ll T$ for short-pulse conditions,

$$\Delta v \;\approx\; \frac{2l}{T} \; . \tag{6}$$

The values of L and l for the beam tubes investigated were about 13 cm and 1 cm, respectively. Then, for example, a pulse period of 1300 μsec would select atoms with a mean velocity v = 100 m/sec and a velocity spread Δv = 15.4 m/sec. The measurement procedure for this short-pulse experiment is as follows:

1. Choose a pulse period commensurate with the range of velocities that are expected.
2. Choose a pulse width less than l/v. As indicated, pulse widths of 20 to 40 μsec were used in our experiments.
3. Sweep the microwave frequency through the center of the Rabi pedestal and over a frequency range equal to several inverse periods $1/T$.
4. Change the pulse period and repeat the sweep with the pulse width kept constant.

Figure 5 shows the results for three pulse periods. For our computations we used the peak-to-valley amplitude of each sweep's Fourier component at the frequency $1/T$. For the 1300-μsec spectrum, the peak-to-valley Ramsey-resonance current component $I_p - I_v$ (hereafter known as I_{pv}) is very nearly equal to $I_p - I_v$ as marked on Figure 5. However, for the 722-μsec data, I_{pv} at $1/722$ μsec is very small, because the spacing of the maxima is close to $1/(2 \times 722$ μsec). The final data set consists of pairs of pulse periods T (with an associated velocity $v \approx L/T$) and peak-to-valley currents I_{pv}.

During the CW operation of the tube, the number of atoms detected near resonance is a convolution over all velocity components and is given by

$$S(\omega - \omega_o) \;=\; \int N(v)\sin^2 2b\tau \cos^2 1/2(\omega - \omega_o)T\,dv \quad , \tag{7}$$

where

$(\omega - \omega_o)$ is the frequency offset from ω_o;

τ represents the transit time through one cavity $(\tau = l/v)$;

T is the time of flight between the cavities $(T = L/v)$;

b is proportional to the microwave field in the cavities and represents the interaction between that field and the Cs atom (b is a constant near resonance);

$N(v)$ = the velocity distribution function; and

$N(v)dv = dN$, the number of detected atoms per second moving with a velocity between v and $v + dv$.
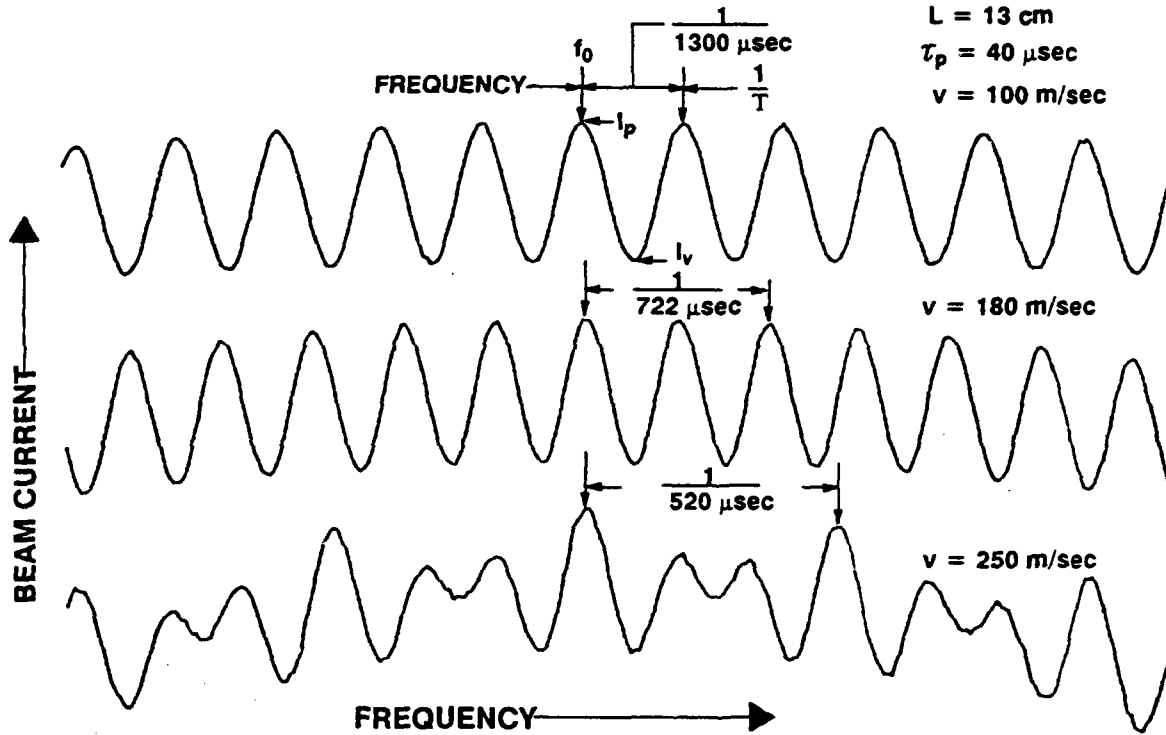
9

Figure 5. Portion of the Ramsey Spectrum Selected by the Pulsed Micro-
wave Condition. The Ramsey pattern for the three different pulse periods
corresponds to three different velocity groups. The fundamental Ramsey
frequency is given by 1/T.

Under the short-pulse conditions, τ is replaced by the fixed pulse width τ_p, with $2b\tau = \pi/2$ for maximum signal. The number of atoms captured in a single pulse period is equal to dN times the length of time it takes the atoms to pass through the interaction region $= dNl/v = N(v)dvl/v$. Because the window width is $2l/T$ and $v = L/T$, we finally obtain the number of atoms captured in a single pulse period, which is $N(v)2l^2/L$. The capture is repeated at every interval T, and leads to an average signal I_{pv} that is given by

$$I_{pv} = \frac{1}{T}N(v)\frac{2l^2}{L} \quad . \tag{8}$$

Hence

$$N(v) = \frac{L}{2l^2}TI_{pv} \quad . \tag{9}$$

In the long-pulse approximation in which $\tau_p \gg l/v$, the number of atoms captured per pulse is $\tau_p dN$. Consequently,

10

$$I_{pv} \approx \left(\frac{\tau_p}{T}\right) dN, \quad \text{where } dN = N(v) \times \frac{2l}{T} \left[1 + \left(\frac{L}{l}\right)\left(\frac{\tau_p}{T}\right) \right]. \tag{10}$$

The normalized velocity distribution $\rho(v)$ for a tube is defined to be $N(v)/N_{max}(v)$ and can be derived from the short-pulse data according to Eq. (11):

$$\varrho(v) = \frac{TI_{pv}(T)}{[TI_{pv}(T)]_{max}} \tag{11}$$

Figure 6 shows the transition from short-pulse to long-pulse operation. The peak signal (about 0.14 nA) evident in the short-pulse regime occurs when $2b\tau_p = \pi/2$, where b is proportional to the square root of microwave power. The long-pulse regime occurs when $\tau_p > l/v$ (≈ 100 μsec) and leads to a signal proportional to $\tau_p \left[1 + \left(\frac{L}{l}\right)\left(\frac{\tau_p}{T}\right) \right]$ [see Eq. (10)]. When the velocity window exceeds the width of the velocity distribution itself, however, the signal becomes proportional to τ_p and tends to the normal CW value.
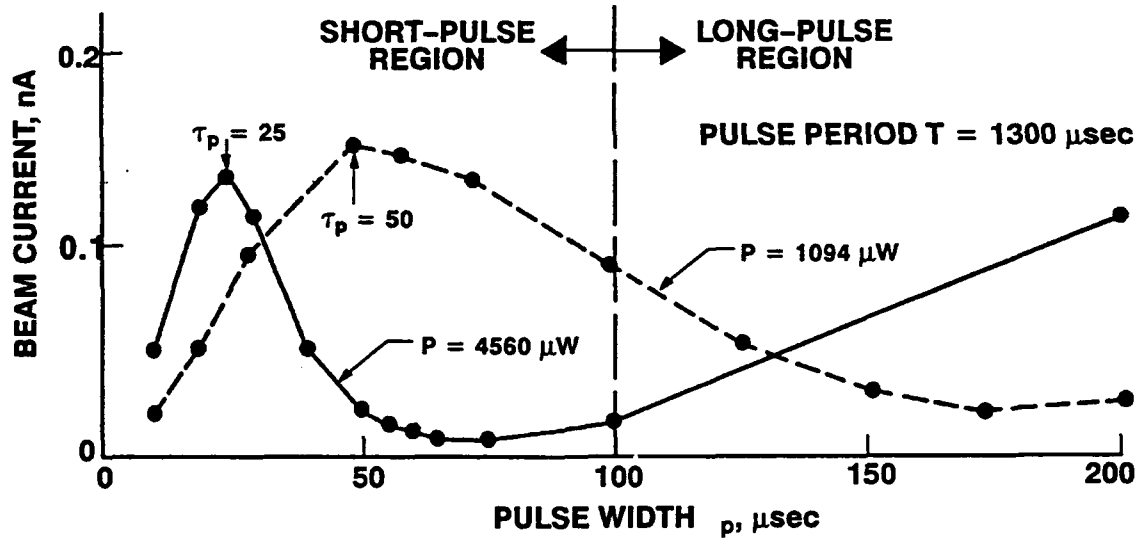
Figure 6. A Plot of the Output of the Cs Beam Tube as a Function of the Pulse Width τ_p for Two Different Microwave Powers

To determine the average velocity from the velocity distribution curve, we calculate as follows:

$$\text{average velocity} = \bar{v} = \frac{\int_0^\infty v\varrho(v)dv}{\int_0^\infty \varrho(v)dv} \tag{12}$$

Figure 7 shows the block diagram of our pulsed microwave measurement system, interfaced to a Hewlett-Packard model 9825 digital computer that is used as a controller and data-

acquisition system. The microwave sweep and the setting of the pulse period are both computer controlled. All of the data necessary to compute the velocity distribution function for a tube are taken automatically and stored on disk. The final data reduction is accomplished by transferring the data to an IBM model 3090 computer.
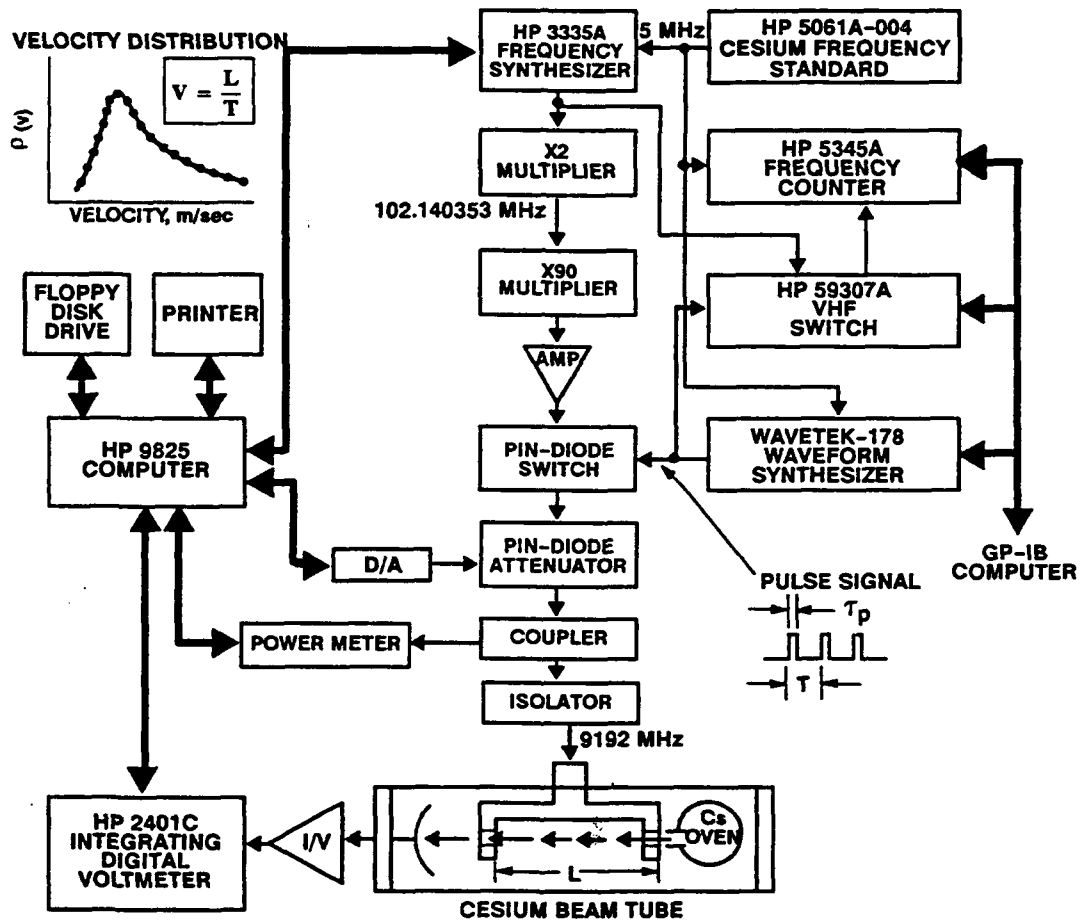

Figure 7. Block Diagram of the System for Measuring the Velocity Distribution of the Cs Beam Tube under Pulsed Microwave Conditions

The peak-to-valley currents that are measured in the pulsed microwave tests are much smaller than the I_{pv} for the CW signal, for two reasons. First, there is a low duty cycle during pulsed operation; second, the measured currents result from only those Cs ions that are within the selected velocity window. These small signals require long integration times to generate acceptable signal-to-noise ratios. Thus, a velocity window of ten percent of the most probable velocity will lead to a signal current of approximately one percent of the CW signal. For a particular Cs beam tube (in this case tube 1), we can see from Figure 6 that when we pulse the microwaves with a pulse width τ_p of 25 μsec and a peak microwave power of about 4560 μW, we then obtain a

12

maximum signal current of 0.14 nA. For each data point the integration time was about two seconds. In this case the CW peak beam current was about 40 nA. For tubes with much lower CW peak currents, the integration time could be as long as five seconds per data point.

For a typical measurement that spans a velocity range of 70 to 240 m/sec, 80 data points per curve are taken, with 101 frequency samples per data point. An integration time of two seconds is used for each data point and a one-second counter-gate time for each frequency measurement. To collect all the raw data required for the velocity distribution curve takes about 6.7 hours; the data are then processed by the IBM 3090 computer and are plotted.

III. RESULTS OF THE VELOCITY DISTRIBUTION MEASUREMENTS

Velocity distribution measurements were performed on six Cs beam tubes from four different manufacturers. Multiple measurements were made on some tubes to determine the reproducibility of the measurements.
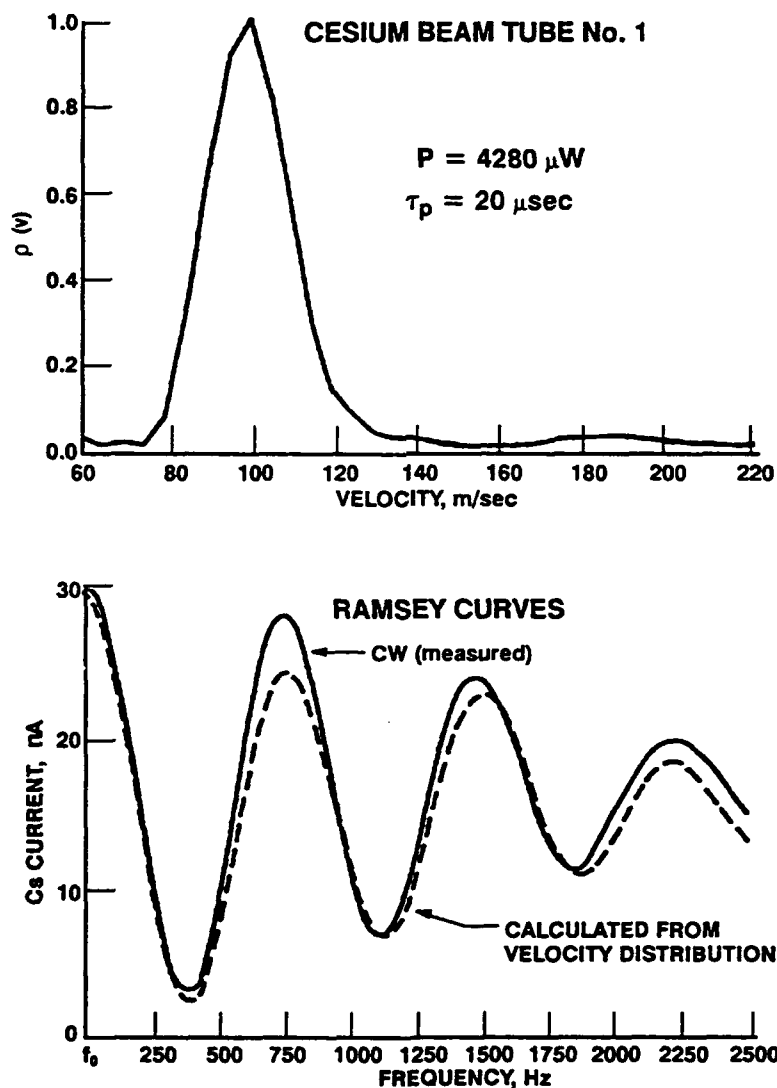

Figure 8. Comparison of the Experimentally Measured Ramsey Pattern under Normal CW Operation with a Pattern Calculated Using the Measured Velocity Distribution of Cs Beam Tube No. 1 (top)

To verify that the velocity distribution that was measured was correct, we calculated the Ramsey resonance curve for tube 1 by using Eq. (7) and the measured velocity distribution; then we compared this calculated curve to the measured Ramsey resonance curve for the tube. Figure 8 shows the measured velocity curve and a comparison between the calculated and measured Ramsey resonance curves. In general, the two Ramsey curves are in close agreement.

Figure 9 shows the plots of the velocity distributions of four other Cs beam tubes. Notice that some of these velocity distribution widths (for tubes 1 and 2) are much narrower than they are for others, indicating that there is a substantial amount of velocity rejection by the beam optics. The wider velocity distributions have Ramsey resonance curves that are broader and more
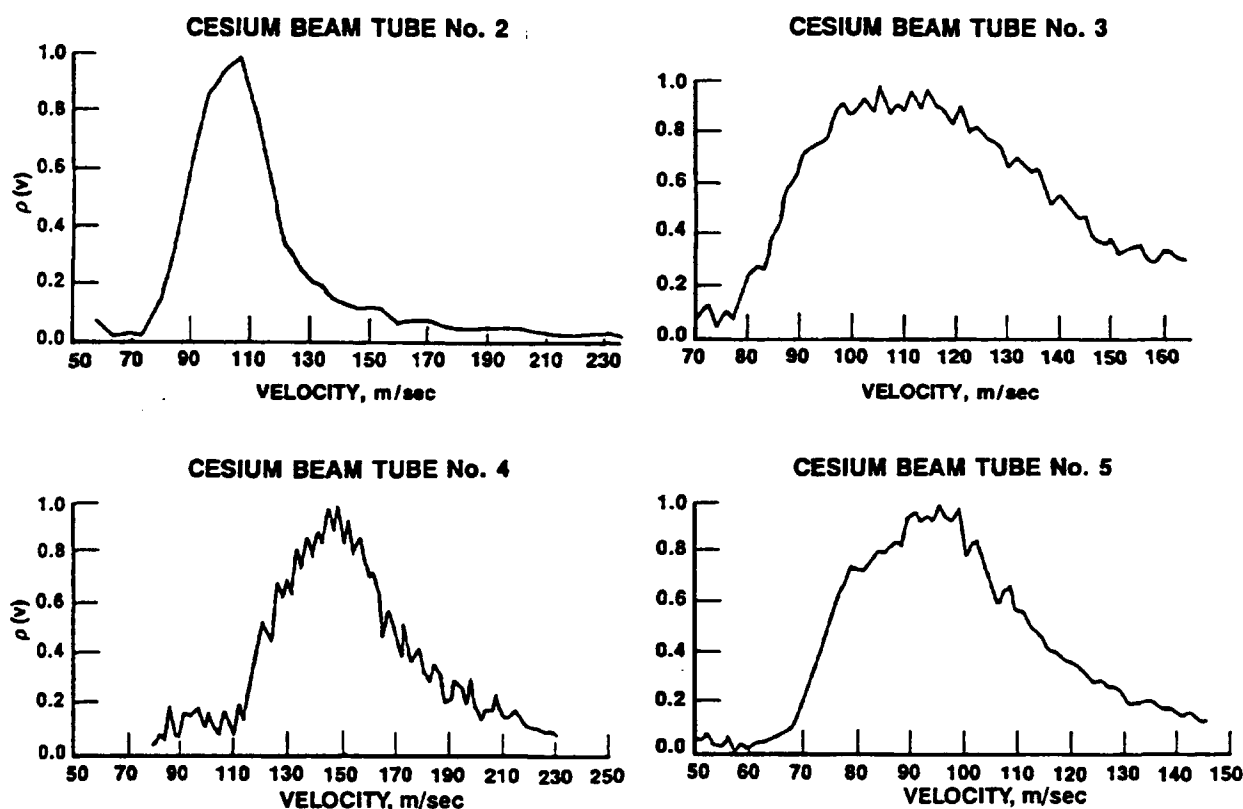

Figure 9. Measured Velocity Distributions for Four Cs Beam Tubes from Four Different Manufacturers

damped. The width of the Ramsey discriminator decreases as the average velocity decreases, and for a fixed average velocity the Ramsey signal increases as the width of the velocity curve increases. Both effects improve the frequency stability of the clock. Note that in some velocity distribution data (e.g. for tube 4 in Figure 9) there appears to be a fine structure in the data. This structure is not really in the velocity distribution, but is caused by contributions from nearby Zeeman transitions [1].

Table 1 summarizes the velocity measurement parameters for five Cs beam tubes. Tubes 1 and 2 are from the same manufacturer and demonstrate the effect of manufacturing tolerances on velocity distributions. The other tubes are from different manufacturers and show the variability of short tube-velocity distributions among different designs. Tubes 1 and 2 were measured more than once, to show the reproducibility of the measurement. The time interval between these measurements was about three days. The table shows the average velocity $\bar{v}$ and the 50% velocity distribution width $\Delta v_{50\%}$; these are tabulated along with estimates of the average velocity from the measured CW Ramsey resonance curve. The CW Ramsey velocity estimate is calculated by averaging the frequency separations of the Ramsey peaks and then multiplying this average frequency separation by the cavity length L to obtain the estimated average velocity for the Cs beam. The results show that the two different methods give answers that are in close agreement. Other parameters are also tabulated, such as the measurement pulse width τ_p, the microwave power, and so on.

Table 1. Measurement Data for Five Cesium Beam Tubes

TUBE No.	CW DATA		PULSED DATA					
	$I_p,$ nA	$I_v,$ nA	$\tau_p,$ sec	$P_{PEAK},$ μW	$\bar{v},$ m/sec	$\Delta v_{50\%},$ m/sec	$\bar{v}_{EST},$ m/sec	$v_{PEAK},$ m/sec
1	40	3.2	40	1000	103.5	23	102	99.9
	40.0	3.2	20	1000	103.1	23	102	99.9
	40.0	3.2	20	4280	108.6	24	102	99.9
2	4.6	1.6	20	1010	116.1	29	113	107.5
	4.6	1.6	20	4050	115.6	30	113	107.5
3	15.7	3.5	35	500	119.0	54	107	108.9
4	5.7	2.1	40	2000	153.0	46	144	149.7
5	207.6	47.9	20	4000	98.4	37	92	95.7

In order to investigate the origin of the Rabi pulling in a sixth Cs beam tube, we measured the individual velocity distributions for each of the Ramsey curves of the seven Cs transitions. This Cs beam tube exhibited Ramsey curves with high signal-to-noise ratios for all of the seven transitions, as shown in Figure 10. Ramsey curves are usually highly attenuated on the outer Zeeman transitions, because C-field inhomogeneities broaden the spectrum. Consequently, this particular tube has a very uniform C-field and permits the measurement to be made.

Figure 11 shows the plots of all seven velocity distributions. The velocity distribution of the main Ramsey transition is shown by itself, but the velocity distributions of the upper and lower Ramsey transitions are superimposed; for example, the velocity distribution of the first higher-frequency transition is compared with that of the first lower-frequency transition, and so on. Note that the higher-frequency velocity distribution is shifted above that of the lower by about 3 to 4 m/sec for each of the pairs. Apart from this shift, we can see that there is very little difference between these paired velocity distributions. This implies that the effects of Rabi pulling

16

should be small. This was confirmed in our earlier study [4], which showed the effects of micro-wave power variation on the output of the standard using this tube, as shown in Figure 12. The maximum frequency offset was only 3×10^{-12} for a $+3$-dB change in microwave power, and the C-field could be changed over a wide range without affecting the standard's dependence on microwave power level.
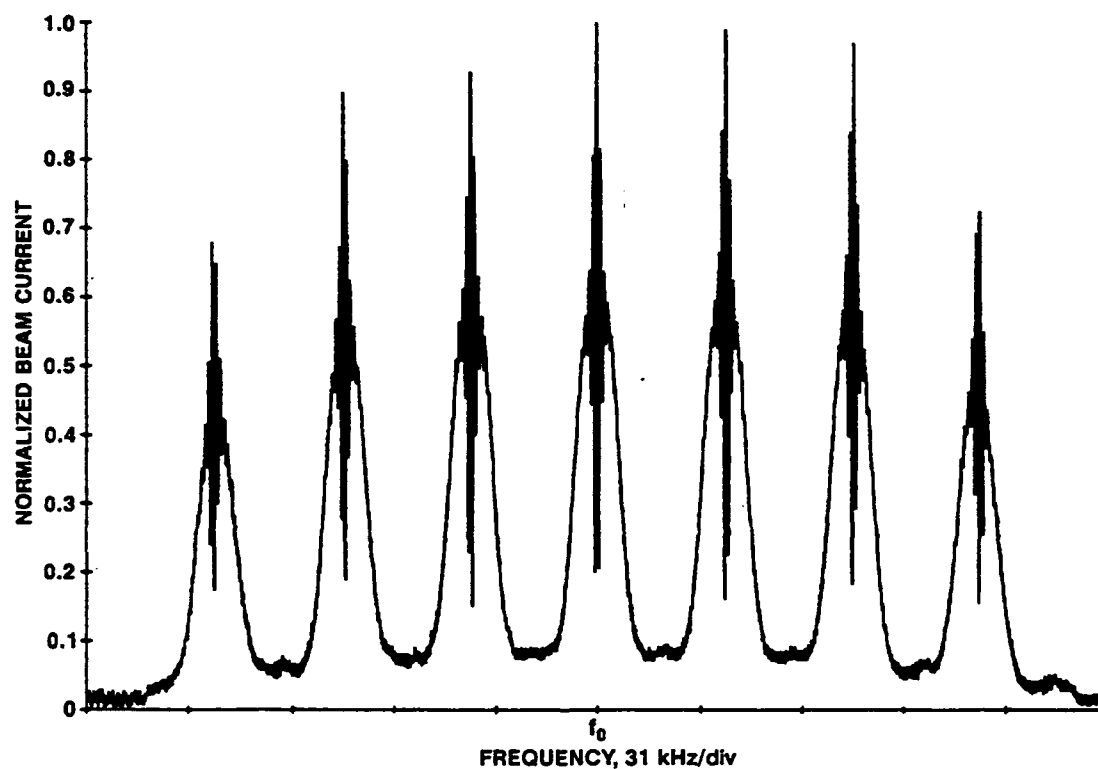

Figure 10. The CW Ramsey Patterns of the Seven Zeeman Transitions in a Cs Beam Tube
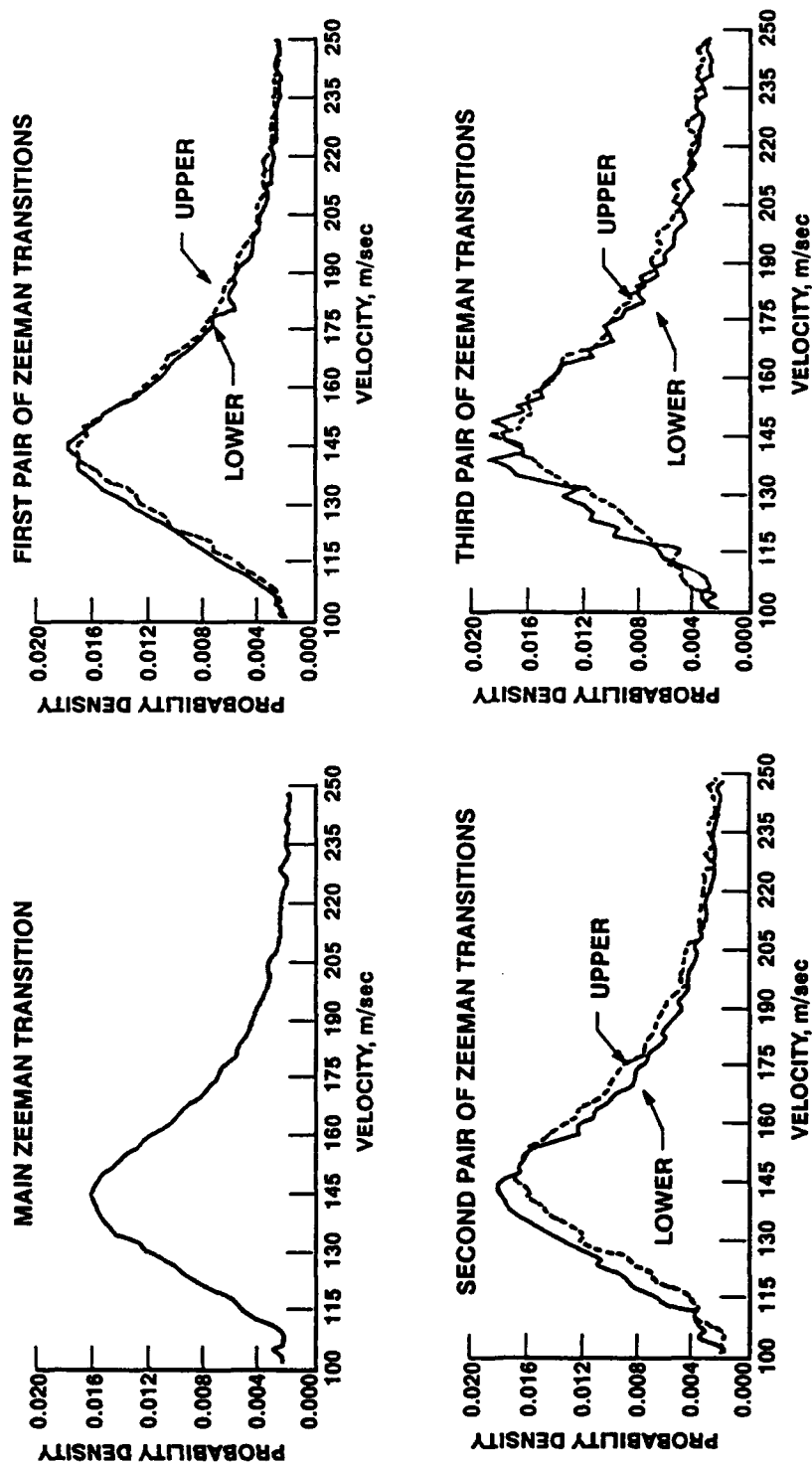
Figure 11. A Plot of All Seven Zeeman-Transition Velocity Distributions, Comparing the Higher-Frequency and Lower-Frequency Velocity Distributions
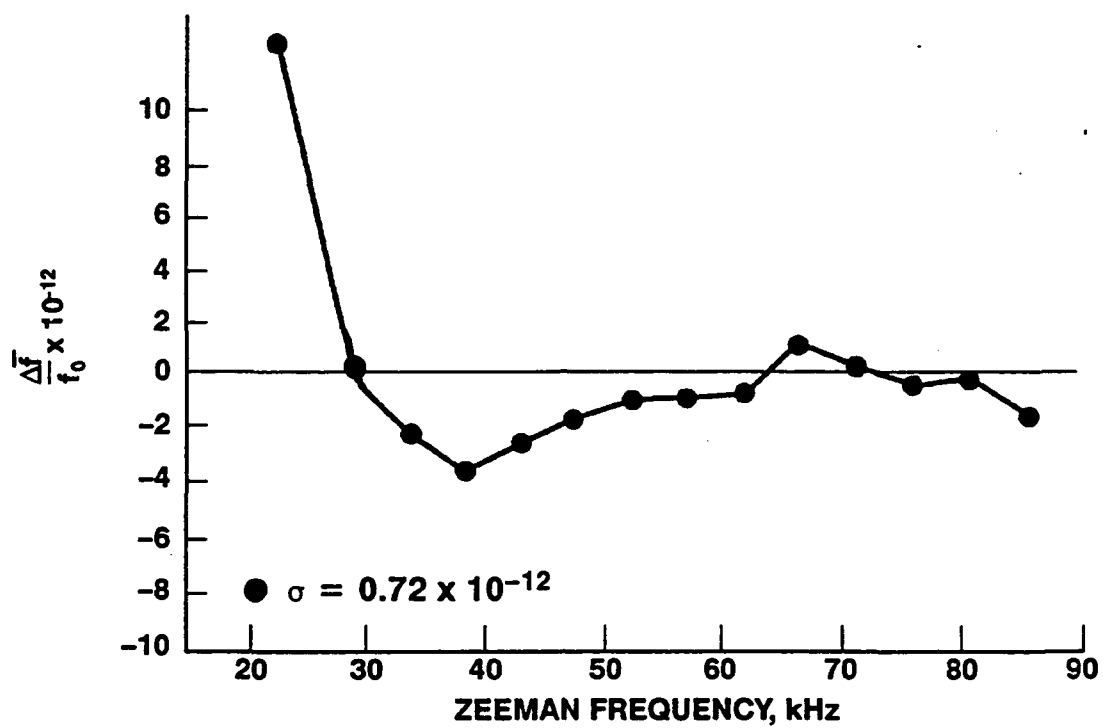
18

Figure 12. A Plot of the Change in Frequency of Cs Standard No. 6 as a
Function of its C-Field for a CW Microwave Power Change of +3 dB above
the Optimum Power Level (the Power Level that Results in Maximum Beam
Current)

IV. SUMMARY

We have constructed an automated pulsed microwave measurement system to measure the velocity distributions of Cs atoms in Cs beam tubes. Measurement data on six Cs beam tubes from four different manufacturers are presented. Computer control enables the data to be collected efficiently and turns this technique into a simple tool for beam tube evaluation. We have illustrated the usefulness of this technique with three examples: (1) a comparison of two tubes taken from the same manufacturer to demonstrate the effect of manufacturing tolerances, (2) a simple comparison of the velocity distributions of tubes from different manufacturers, and (3) a measurement of velocity distributions for different Zeeman transitions and the correlation of those distributions with Rabi pulling. The technique augments other methods for characterizing beam tubes, and can help in the selection of criteria for acceptable velocity distributions.

REFERENCES

1. H. Hellwig, S. Jarvis, D. Halford, and H. E. Bell, "Evaluation and operation of atomic beam tube frequency standards using time domain velocity selection modulation," *Metrologia*, vol. 9, pp. 107–112, 1973.

2. H. Hellwig, S. Jarvis, D. J. Glaze, D. Halford, and H. E. Ball, "Time domain velocity selection modulation as a tool to evaluate cesium beam tubes," in *Proceedings of the 27th Annual Symposium on Frequency Control* (Ft. Monmouth, N. J.), pp. 356–362, June 1973.

3. D. A. Howe, H. E. Bell, H. Hellwig, and A. DeMarchi, "Preliminary research and development of cesium beam tube accuracy evaluation system," in *28th Annual Symposium on Frequency Control*, pp. 362–372, 1974.

4. S. K. Karuza, W. A. Johnson, J. P. Hurrell, and F. J. Voit, "Determining optimum C-field settings that minimize output frequency variations in cesium atomic frequency standards," in *21st Annual Precise Time and Time Interval (PTTI) Applications and Planning Meeting* (Redondo Beach, Calif.), November 1989.